



Experimental Investigation of
Radar Cross Section Spatial Correlation Properties
for a Point Scattering Target

THESIS
John David Shannon
Second Lieutenant, USAF

AFIT/GE/ENG/96D-19

DISTRIBUTION STATEMENT A

Approved for public release,
Distribution Unlimited

DEPARTMENT OF THE AIR FORCE
AIR UNIVERSITY
AIR FORCE INSTITUTE OF TECHNOLOGY

Wright-Patterson Air Force Base, Ohio

DTIC QUALITY INSPECTED 3

19970128 301

AFIT/GE/ENG/96D-19

Experimental Investigation of
Radar Cross Section Spatial Correlation Properties
for a Point Scattering Target

THESIS
John David Shannon
Second Lieutenant, USAF

AFIT/GE/ENG/96D-19

Approved for public release; distribution unlimited

The views expressed in this thesis are those of the author and do not reflect the official policy or position of the Department of Defense or the U. S. Government.

AFIT/GE/ENG/96D-19

Experimental Investigation of
Radar Cross Section Spatial Correlation Properties
for a Point Scattering Target

THESIS

Presented to the Faculty of the School of Engineering
of the Air Force Institute of Technology
Air University

In Partial Fulfillment of the
Requirements for the Degree of
Master of Science in Electrical Engineering

John David Shannon, BSEE
Second Lieutenant, USAF

December, 1996

Approved for public release; distribution unlimited

Acknowledgements

I would like to take this opportunity to thank all those people who made this thesis possible. First of all, I want to thank Dr. Byron Welsh, who gave me guidance and motivation. His patience with all of my questions helped me keep going. I would also like to thank my committee, Maj Gerald Gerace and Dr. Andrew Terzuoli, for sharing their knowledge and experience with me.

Since this was an experimental thesis, I had a lot of lab work to do in the anechoic chamber. I want to thank Capt Mike Proudfoot for his support and help with my work in the chamber.

Next, I wish to thank my fellow students for their support in every aspect of my life at AFIT. I want to thank the GE students for their help with my academic life, and my GCS buddies for the less stressful side of AFIT.

Last but not least, I want to thank Weez, who gave me support when I needed it, along with a chance to laugh and have fun. Her time and dedication has meant a lot to me. AFIT should not be experienced in isolation, and I greatly appreciate all the support I received during my AFIT experience from fellow students, professors, and friends.

John David Shannon

Table of Contents

	Page
Acknowledgements	ii
List of Figures	vi
List of Tables	vii
Abstract	viii
 I. Introduction	 1-1
1.1 Motivation	1-1
1.2 Previous efforts	1-5
1.3 Goals	1-7
1.4 Thesis overview	1-7
 II. Theory based autocovariance estimates	 2-1
2.1 Need for theory	2-1
2.2 Requirements	2-1
2.3 Development	2-1
2.4 Sample theoretical autocovariance calculation	2-4
 III. Measurement Procedure	 3-1
3.1 Motivation for Static Measurements	3-1
3.2 Generating Data Based Autocovariance	3-1
3.3 Setting Up the Static Measurements	3-2
 IV. Results	 4-1
4.1 Data Matrix	4-1
4.2 Varying Number of Scatterers	4-1
4.2.1 Motivation for Varying Number of Scatterers	4-1

	Page
4.2.2 How to Make the Measurements	4-2
4.2.3 Expected Results	4-2
4.2.4 Results	4-3
4.3 Varying Target Size	4-5
4.3.1 Motivation for Varying Target Size	4-5
4.3.2 How to Make the Measurements	4-5
4.3.3 Expected Results	4-6
4.3.4 Results	4-6
4.4 Varying Spacing Between Scatterers	4-8
4.4.1 Motivation for Varying Spacing Between Scatterers	4-8
4.4.2 How to Make the Measurements	4-8
4.4.3 Expected Results	4-9
4.4.4 Results	4-9
4.5 Summary	4-12
V. Conclusions and Recommendations	5-1
5.1 Conclusions	5-1
5.2 Recommendations	5-2
Appendix A. Specifications for the AFIT anechoic chamber	A-1
A.1 Specifications	A-1
Appendix B. Data Collection Procedure	B-1
B.1 Generating scattering locations	B-1
B.2 Taking data	B-1
B.3 Data preparation	B-2
B.4 Finding autocovariance	B-3
B.5 Taking average of autocovariances	B-4
B.6 Predicting autocovariance	B-4

	Page
B.7 Plotting comparisons	B-4
B.8 Figures of merit	B-4
Bibliography	BIB-1
Vita	VITA-1

List of Figures

Figure		Page
1.1.	Radar Receiver Output PDF	1-2
1.2.	Sample RCS measurement range	1-4
1.3.	Outlines of Noble's target scatterer pdf models	1-8
2.1.	Sample Radar Geometry Setup	2-2
2.2.	Theoretical Autocovariance (ACV) for 30λ square target, 50 scatterers.	2-5
3.1.	Static measurement setup - styrofoam with thin cylinders placed on grid.	3-3
3.2.	Sample RCS azimuth sweep - 100 scatterers, 30λ square	3-3
3.3.	Sample data based autocovariance estimate	3-4
3.4.	Main lobe of sample autocovariance	3-5
4.1.	10 scatterers, 30λ square, average of 10 realizations	4-4
4.2.	50 scatterers, 30λ square, average of 9 realizations	4-4
4.3.	200 scatterers, 30λ square, average of 10 realizations	4-5
4.4.	50 scatterers, 14λ square, average of 10 realizations	4-6
4.5.	50 scatterers, 30λ square, average of 9 realizations	4-7
4.6.	50 scatterers, 36λ square, average of 10 realizations	4-7
4.7.	Target scatterer distribution for validating independence of scatterers.	4-8
4.8.	9 scatterers, 3λ square, 1 realization	4-10
4.9.	9 scatterers, 12λ square, 1 realization	4-10
4.10.	9 scatterers, 18λ square, 1 realization	4-11
4.11.	9 scatterers, 30λ square, 1 realization	4-11
4.12.	9 scatterers, 36λ square, 1 realization	4-12
B.1.	Example scattering locations generated from matlab for 200 scatterers	B-2

List of Tables

Table		Page
4.1.	Data matrix of static measurements used to characterize and validate theoretical autocovariance predictions	4-1
4.2.	FWHM when varying the number of scatterers	4-3
4.3.	FWHM when varying target size	4-6
4.4.	9 discrete point scatterer test frequencies and spacing	4-9
4.5.	FWHM when varying spacing between scatterers	4-9
5.1.	Effects of varying density of scatterers on ACV main lobe	5-1

Abstract

This research investigates the spatial correlation of RCS. In pulsed radar systems, probability of detection for partially correlated signals depends on the autocovariance of the target's RCS. The RCS changes pulse to pulse due to spatial and time fluctuations. Spatial fluctuation are due to the motion of all scatterers relative to the radar (i.e. changing aspect angle). Time fluctuations are due to relative motion of scatterers to each other (i.e. wings flexing, engines spinning). Theory developed at AFIT (9) can generate autocovariance estimates from a distribution of scatterers. Theory based autocovariance estimates are compared to static measurement based autocovariance estimates in order to validate this theory. Interaction among scatterers is the most significant source of deviation between theory and measurement based autocovariance estimates.

Experimental Investigation of
Radar Cross Section Spatial Correlation Properties
for a Point Scattering Target

I. Introduction

1.1 Motivation

In both the military and civilian sectors, radar systems are used to detect the presence of aircraft, as well as to track them. A radar sends out a signal and determines if a target is present based on the return it receives. This return power is a function of the Radar Cross Section (RCS)(1). The RCS is defined as follows:

$$\sigma = \lim_{r \rightarrow \infty} 4\pi r^2 \frac{|E_s|^2}{|E_i|^2}, \quad (1.1)$$

where

σ Radar Cross Section, m²,

r Distance from radar to target, m,

E_s Scattered electric field, V/m,

E_i Incident electric field, V/m,

RCS is proportional to the amount of power scattered back towards the radar. The radar engineer needs a way to accurately characterize the RCS statistics in order to determine the probability of detection (P_D) for the aircraft.

The Neyman Pearson criteria is used to find P_D for a radar system. First, an acceptable probability of false alarm, P_{FA} is determined. The threshold voltage of the radar, V_t is found from

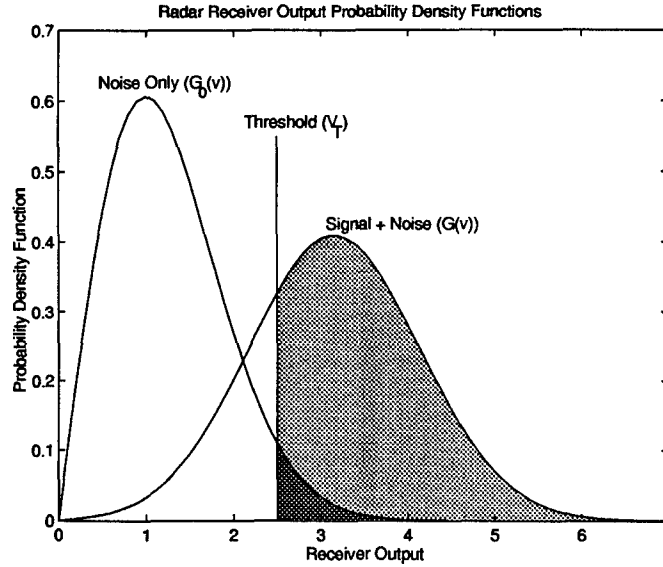


Figure 1.1 Radar Receiver Output PDF

$$P_{FA} = \int_{V_t}^{\infty} G_o(v)dv, \quad (1.2)$$

where $G_o(v)$ is the probability density function of noise.

The probability of detection is

$$P_D = \int_{V_t}^{\infty} G(v)dv, \quad (1.3)$$

where $G(v)$ is the probability density function of signal plus noise in the system.

In order to characterize the RCS pdf, we must view the RCS in terms of dynamic RCS, the RCS of an aircraft in flight. RCS is not one single number for a given target. Instead, RCS is a function of frequency, target geometry, polarization, and angle of observation. The frequency and polarization are attributes of the incident wave. Even if we know the aspect angle and target geometry, we may not necessarily be able to calculate the dynamic RCS. Time effects, such as wings flexing and engines spinning, lead to a fluctuating RCS for a given angle of observation.

Time variations are the result of the relative motion of individual scatterers with respect to each other. It makes more sense to treat RCS statistically as a function of time, $\sigma(t)$, with some mean and correlation function.

To extend the idea of a fluctuating RCS, consider pulsed radars. These radars integrate many pulses to increase the signal to noise ratio and thus, increase P_D . If every pulse has the same RCS return, there is said to be 100% pulse to pulse correlation. Probability of detection is easy to calculate in this case. No fluctuation of RCS is present and we can substitute the RCS plus noise pdf directly into Eqn. (1.3). Pulse to pulse correlation will not be 100% due to time varying effects though. In addition, we also have to consider RCS fluctuations due to spatial effects. Spatial variations are the result of the relative motion of all scatterers with respect to the radar, i.e. the target is changing aspect angle during the pulse integration period. What we need to know is the mean RCS and correlation as a function of space and time, $\sigma(\hat{r}, t)$, where \hat{r} is the observation direction and t is the time of observation.

If we know the distribution of signal and noise, $G(v)$, calculating P_D is straightforward. The problem is in knowing this distribution. Due to the time and spatial fluctuations discussed above, $G(v)$ is best characterized by a distribution that takes into account the pulse to pulse correlation. Swerling developed distributions for 100% and 0% pulse to pulse correlation (8). The difficulty lies in computing $G(v)$ for a pulse to pulse correlation that is not 100% or 0%. In order to calculate a distribution, $G(v)$, for a pulse to pulse correlation between 100% and 0%, two things must be known: the correlation coefficient, or how fast the RCS decorrelates in space and time, and the rate at which the aircraft is changing aspect angle. This research only deals with the spatial correlation coefficient, or autocovariance, and not the time autocovariance or the aircraft's turning rate. We need the normalized autocovariance $\rho_\sigma(\hat{r}, t)$ to find P_D ¹.

¹See chapter 2 for discussion on the how to calculate $\rho_\sigma(\hat{r}, t)$

One way to estimate the autocovariance is from a static RCS measurement. Static measurements are performed on a fixed target, usually on a scaled model in an anechoic chamber. The target is placed on a pedestal and a radar transmitter sends an incident field, which is scattered by the target. Figure 1.2 shows a sample RCS measurement setup. Some of the energy reaches

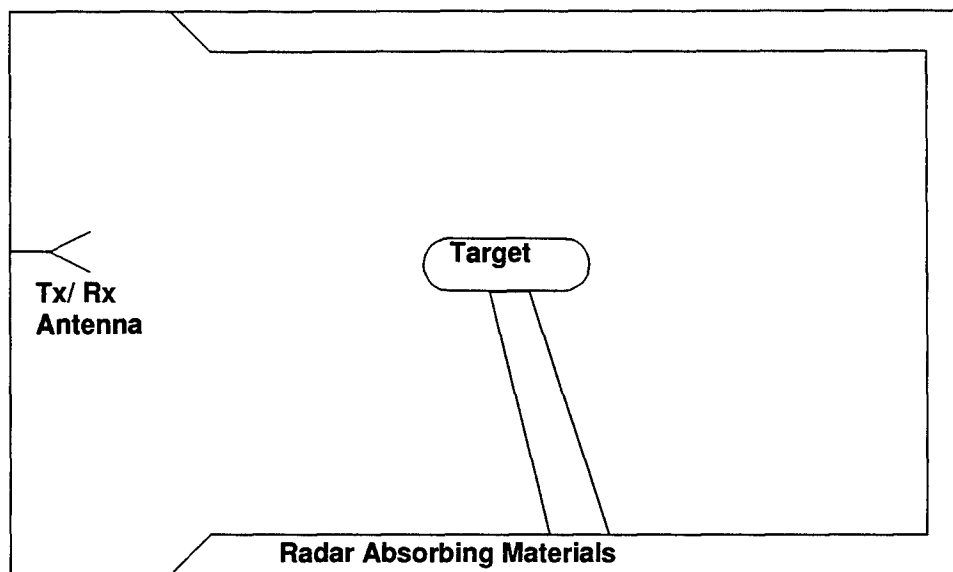


Figure 1.2 Sample RCS measurement range

the receiving antenna as the scattered field and thus, RCS can be calculated for a given frequency and angle of observation. This number is repeatable and deterministic, but an aircraft in flight will not have a deterministic RCS at a given angle of observation and frequency. Due to moving parts on the aircraft, the RCS will deviate slightly from the static measurement. This deviation will be small, so we can treat the static RCS measurement as the average RCS, where the fluctuations cause the RCS to vary around this average. The target can be rotated over 360 degrees of azimuth. Static measurements are a good way to determine average RCS for any given angle of observation, but we still need the correlation to determine the target return pdf, $G(v)$. An autocovariance estimate from static data only includes spatial effects, and not time effects, since no scatterers are moving relative to each other. From static measurements we can get spatial correlation, but not time correlations.

One way to account for both the spatial and time effects is to take the autocovariance of dynamic data. In this case, a real aircraft is flown against a radar. Dynamic measurements are of limited value in the design phase of an aircraft since the aircraft has to be built and flown. Even when we consider a working aircraft, some problems arise. The process of measuring dynamic RCS is time consuming and expensive. In addition, much more data is generated than in the static case and storage of all this data is a concern.

The ideal situation would be to somehow generate the RCS autocovariance without having to build the aircraft or even a model, without having to pay the cost and time of flying the aircraft, and without having to store large amounts of data. Theory developed at AFIT promises to fulfill all these goals (9). The theory provides a way to generate the second order statistics of a distribution of scatterers. The following are assumptions of the theory:

1. The target is composed of independent scattering centers.
2. The phase of all scatterers is uniformly distributed over $[0, 2\pi]$.

In addition, the autocovariance can be characterized based on these parameters:

1. Target size relative to wavelength.
2. Number of scattering centers in target.

This research effort investigates the effects of these assumptions and characteristics.

1.2 Previous efforts

This research is a follow on to four previous efforts at AFIT. Buterbaugh completed the earliest work in 1992 (2). He established the relevance of pulse to pulse correlation of the radar returns to probability of detection. In addition, he determined the RCS statistics could be characterized without knowing the complete details of the target geometry. His results confirmed that the statistical model developed by Welsh could be used in the calculation of probability of detection.

Fischer continued the work in 1992. He compared the theoretical autocovariance estimations to autocovariance estimations generated from dynamic data for an unspecified aircraft at broadside and nose-on. In the broadside case, very few time fluctuations in RCS occur, while at nose on, jet engine modulation (JEM) is present. He concluded that predicted statistics and data generated statistics were similar enough to warrant further research (3).

The research was continued by Kehr, who looked at more angles than just broadside and nose on. He acquired dynamic data taken at Patuxent River, Maryland of a C-29 aircraft. Autocovariance curves were generated from dynamic data. These autocovariance curves were compared to theory based autocovariance curves. He started with a target distribution model, which is a pdf of scatterers that represents the target. The distribution can be used in the theory to generate an autocovariance. Kehr used a uniform distribution of scatterers and an ISAR (Inverse Synthetic Aperture Radar) image. The uniform model was generated by creating a rectangular volume with the maximum dimensions equivalent to the aircraft dimensions in terms of wavelengths and filling it with a uniform distribution of scatterers. The ISAR image is a high fidelity model of the scattering centers created from a radar image of the static model. Both of these distributions were used to generate autocovariance estimates which were then compared to the dynamic data based estimates. Kehr expected and found that the more accurate model (ISAR) produced autocovariance estimates that more closely resemble the dynamic statistics (4). These factors led to Noble's research.

In 1994, Noble examined 9.2GHz RCS data on the C-29 and compared it to five different distributions of scatterers instead of only two (7). At this frequency, the large target assumption is more valid. The five models he used are listed below, and shown in Fig. 1.3.

1. *Rect* – The same as Kehr's uniform model
2. *Multi-Rect* – A box overlay of the aircraft with a uniform distribution of scatterers throughout
3. *Silhouette 1* – Outline of the aircraft with uniform distribution of scatterers
4. *Silhouette 2* – Outline of aircraft with scatterers placed more densely on engine areas

5. *ISAR* – High fidelity radar image of target

Each of these distributions was used to generate autocovariance curves that were compared to dynamic data generated statistics. Higher fidelity models yielded autocovariance curves that more closely resemble dynamic data based autocovariance curves.

1.3 *Goals*

The theory has not been characterized and validated. All of the past research efforts assumed the theory can accurately generate the autocovariance sequence for a given distribution of scatterers. This research investigates the effect of varying the following three parameters of the theory.

1. *Number of scatterers.*
2. *Target size with respect to wavelength.*
3. *Spacing between scatterers.*

This research examines the effects of these parameters by varying each in static measurements and comparing the resulting autocovariance curves to predicted results.

1.4 *Thesis overview*

Chapter 2 describes the theory along with a brief review of its mathematical development. A simple example is presented to show how knowing the target scatterer distribution leads to autocovariance.

Chapter 3 describes the static measurement procedure used to generate RCS data. This RCS data leads to a data based autocovariance. A simple measurement is presented.

Chapter 4 includes all the data measurements taken, along with comparisons to predicted autocovariance results.

Chapter 5 summarizes the conclusions and provides recommendations for further research.

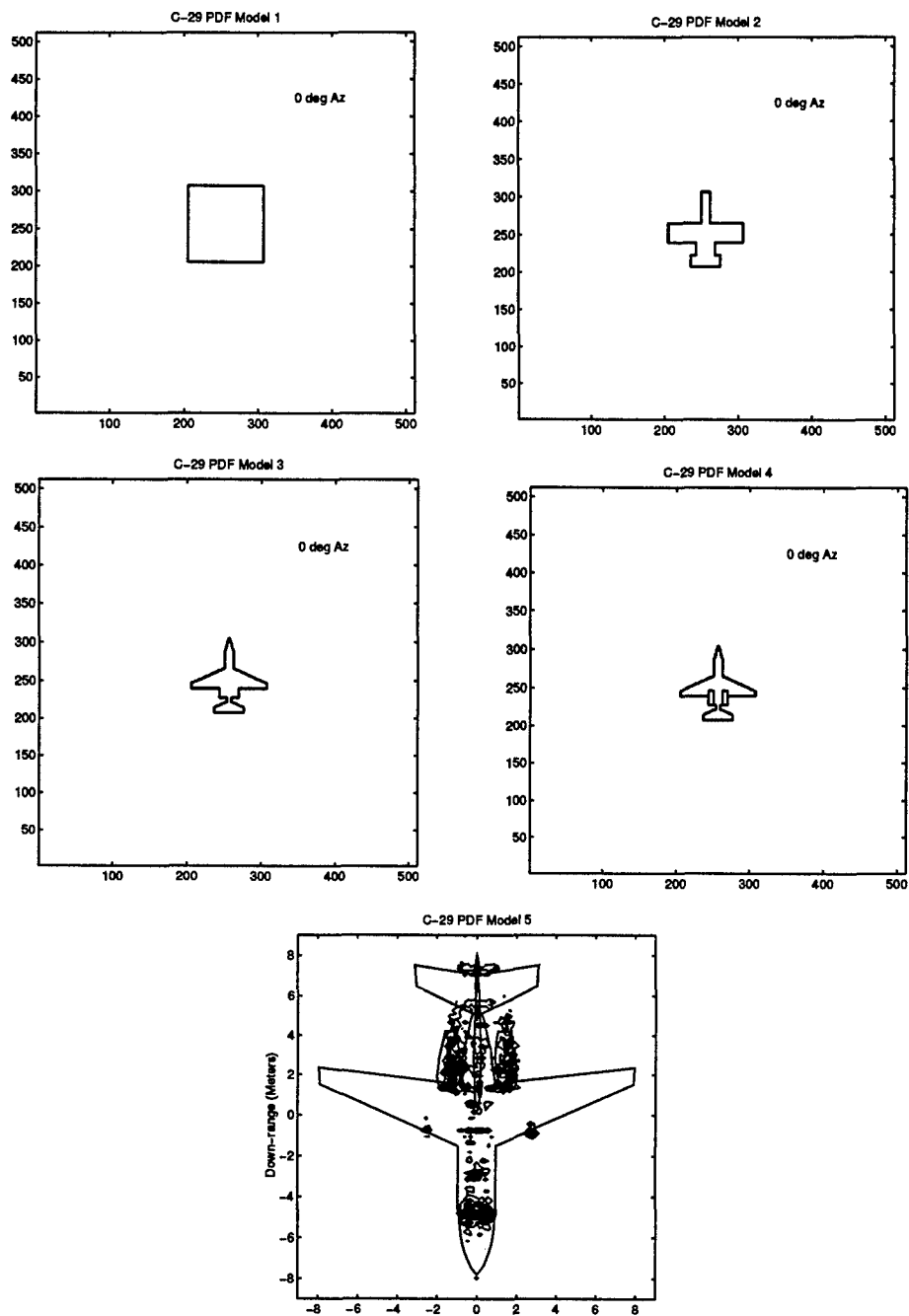


Figure 1.3 Outlines of Noble's target scatterer pdf models

II. Theory based autocovariance estimates

2.1 Need for theory

We want to characterize the RCS fluctuations using the autocovariance. Theory developed at AFIT (9) can generate the autocovariance from a distribution of scatterers. The following chapter shows how we can get autocovariance from the scatterer distribution and what we need to calculate this autocovariance. A sample calculation is presented in section 2.4.

2.2 Requirements

To get any covariance, we need two items to correlate. In this case we want a correlation of two RCS samples. In general these samples will vary in time and space. Later we will make a simplification to include only the spatial correlation, since that is the only effect we can examine in a static measurement.

2.3 Development

Given a setup as shown in Fig. 2.1, the scattered field at one instant in time can be written as

$$y(t, \hat{r}_r, \hat{r}_t) = \sum_{i=1}^N b_i(\hat{r}_r, \hat{r}_t) e^{j \frac{2\pi}{\lambda} (\hat{r}_r + \hat{r}_t) \cdot \vec{r}_i(t)}, \quad (2.1)$$

where N is the number of scatterers, $b_i(\hat{r}_r, \hat{r}_t)$ is the complex reflected field, λ is the wavelength, \hat{r}_t is the unit vector pointing in the direction of the radar transmitter, \hat{r}_r is the unit vector pointing in the direction of the radar receiver, and \vec{r}_i is the vector location of the i^{th} scatterer. In a monostatic measurement, $\hat{r}_r = \hat{r}_t$. Letting $2\hat{r} = \hat{r}_r + \hat{r}_t$, we have $\hat{r} = \hat{r}_r = \hat{r}_t$. From Eqn. (1.1), the RCS can be written as

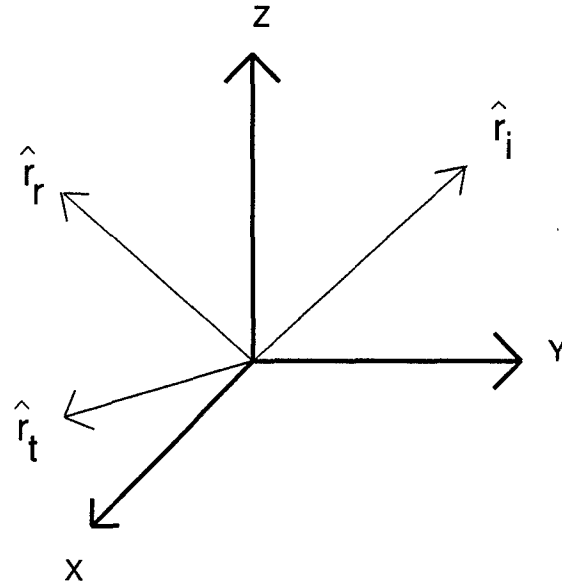


Figure 2.1 Sample Radar Geometry Setup

$$\sigma(t, \hat{r}) = \lim_{r \rightarrow \infty} 4\pi r^2 \frac{|y(t, \hat{r})|^2}{|E_i|^2}, \quad (2.2)$$

For every pulse, E_i and r are the same so

$$\sigma(t, \hat{r}) \propto |y(t, \hat{r})|^2. \quad (2.3)$$

The autocorrelation is given by

$$R_\sigma(t_1, t_2; \hat{r}_1, \hat{r}_2) = E[\sigma(t_1, \hat{r}_1)\sigma(t_2, \hat{r}_2)] \quad (2.4)$$

and the covariance is

$$C_\sigma(t_1, t_2; \hat{r}_1, \hat{r}_2) = R_\sigma(t_1, t_2; \hat{r}_1, \hat{r}_2) - \bar{\sigma}_{incoh}(t, \hat{r}_1)\bar{\sigma}_{incoh}(t, \hat{r}_2), \quad (2.5)$$

where

$$\bar{\sigma}_{incoh}(\hat{r}) = \sum_{i=1}^N E[|b_i(\hat{r})|^2] \quad (\text{incoherent limit}). \quad (2.6)$$

$\sigma_{incoh}(\hat{r})$ is the average RCS assuming $E[b_i(\hat{r})] = 0$, or that the phase of any single scatterer can take on any value from $[0, 2\pi]$ with equal probability. Time dependence is removed when we have a large target volume ($\lambda \ll L$) in a monostatic situation. Normalizing to one, the correlation coefficient or autocovariance is

$$\rho_{\sigma}(t_1, t_2; \hat{r}_1, \hat{r}_2) = \frac{C_{\sigma}(t_1, t_2; \hat{r}_1, \hat{r}_2)}{(C_{\sigma}(t_1, t_1; \hat{r}_1, \hat{r}_1) C_{\sigma}(t_2, t_2; \hat{r}_2, \hat{r}_2))^{\frac{1}{2}}}. \quad (2.7)$$

Recall that we are concerned only with spatial fluctuations since these are the only effects that we can verify with a static measurement. Letting $t = t_1 = t_2$ and simplifying,

$$\begin{aligned} \rho_{\sigma}(t, \Delta\hat{r}) &= \sum_{i=1}^N \frac{\bar{\sigma}_i(\hat{r}_1)}{\bar{\sigma}_{incoh}(\hat{r}_1)} \frac{\bar{\sigma}_i(\hat{r}_2)}{\bar{\sigma}_{incoh}(\hat{r}_2)} \left(1 - \left| M_{\Sigma\hat{r}_i} \left(\frac{4\pi}{\lambda} \Delta\hat{r} \right) \right|^2 \right) \\ &+ \left| \sum_{i=1}^N \left[\left(\frac{\bar{\sigma}_i(\hat{r}_1)}{\bar{\sigma}_{incoh}(\hat{r}_1)} \frac{\bar{\sigma}_i(\hat{r}_2)}{\bar{\sigma}_{incoh}(\hat{r}_2)} \right)^{\frac{1}{2}} M_{\Sigma\hat{r}_i} \left(\frac{4\pi}{\lambda} \Delta\hat{r} \right) \right] \right|^2, \end{aligned} \quad (2.8)$$

where σ_i is the RCS of the i^{th} scatterer, $\Delta\hat{r} = \hat{r}_2 - \hat{r}_1$, and $M_{\Sigma\hat{r}_i}$ is the characteristic function of the scattering location pdf. A complete derivation with all relevant simplifications is given in (9). $\frac{\bar{\sigma}_i(\hat{r})}{\bar{\sigma}_{incoh}(\hat{r})}$ is the ratio of the i^{th} scatterer to the total average return. For equal amplitude independent scatterers, $\frac{\bar{\sigma}_i(\hat{r})}{\bar{\sigma}_{incoh}(\hat{r})} = \frac{1}{N}$ since $\bar{\sigma}_i(\hat{r})$ is the RCS return from the i^{th} scatterer and $\bar{\sigma}_{incoh}(\hat{r})$ is the total RCS return. Substituting this ratio into Eqn. (2.8),

$$\rho_{\sigma}(t, \Delta\hat{r}) = \frac{1}{N^2} \sum_{i=1}^N \left(1 - \left| M_{\Sigma\hat{r}_i} \left(\frac{4\pi}{\lambda} \Delta\hat{r} \right) \right|^2 \right) + \left| \frac{1}{N} \sum_{i=1}^N M_{\Sigma\hat{r}_i} \left(\frac{4\pi}{\lambda} \Delta\hat{r} \right) \right|^2. \quad (2.9)$$

This is the result we want. In addition to the assumptions included in the theory of scatterer independence and mean phase return of zero, we have made the simplifications of equal amplitude scattering centers and spatial effects only. The wavelength is found from $\lambda = \frac{c}{f}$, where f is the frequency of the incident wave and c is the speed of light. The only unknowns are $\Delta\hat{r}$ and the

characteristic function. $\Delta\hat{r}$ is the independent variable. The characteristic function comes directly from the target scatterer pdf in the equation

$$M_{\Sigma\hat{r}_i}(\vec{x}) = \int d\vec{r} p_{\hat{r}_i}(\vec{r}) e^{j\vec{x}\cdot\vec{r}}, \quad (2.10)$$

where $p_{\hat{r}_i}(\vec{r})$ is the pdf of the scattering center locations.

To illustrate the significance of the autocovariance main lobe on pulse to pulse correlation, consider the following. If the spatial autocovariance with respect to angle of an aircraft is a delta function, then any change in aspect angle would lead to a new RCS that would have no relation to the previous RCS return and we have 0% pulse to pulse correlation. If the main lobe of the autocovariance is a constant, 1, RCS returns would be the same for any aspect angle and we have a 100% pulse to pulse correlation. Now consider two aircraft changing aspect angle with respect to a radar at the same rate. The target with a wider autocovariance main lobe would have a higher pulse to pulse correlation than the target with a narrower autocovariance main lobe. We need the autocovariance main lobe along with the aircraft's rate of change to determine the pulse to pulse correlation. This pulse to pulse correlation gives us the shape of the target return distribution. Noise is known, and now we have $G(v)$, which we can integrate to get P_D . The main point of this discussion is when wavelength, number of scatterers, and scatterer pdf are known, a theoretical autocovariance can be calculated, and this autocovariance leads to P_D .

2.4 Sample theoretical autocovariance calculation

Given:

1. Uniform distribution of scatterers in a 2D box 30λ by 30λ . This is a 2D rect function.
2. 50 scatterers
3. $f=15\text{GHz}$, $\lambda=2\text{cm}$

The characteristic function is a spatial Fourier transform of the target scatterer distribution. $M_{\Sigma \hat{r}_i}(\tilde{x}) = \text{sinc}(60\Delta\hat{r}_x)\text{sinc}(60\Delta\hat{r}_y)$ where $\text{sinc}(x) = \frac{\sin(\pi x)}{\pi x}$ and $\Delta\hat{r}_x, \Delta\hat{r}_y$ are the changes in observation direction on the x and y axes. Substituting this characteristic function along with the number of scatterers, 50, into Eqn. (2.9)

$$\rho_\sigma(t, \Delta\hat{r}) = \frac{1}{50^2} \sum_{i=1}^{50} \left(1 - |\text{sinc}(60\Delta\hat{r}_x)\text{sinc}(60\Delta\hat{r}_y)|^2 \right) + \left| \frac{1}{50} \sum_{i=1}^{50} \text{sinc}(60\Delta\hat{r}_x)\text{sinc}(60\Delta\hat{r}_y) \right|^2$$

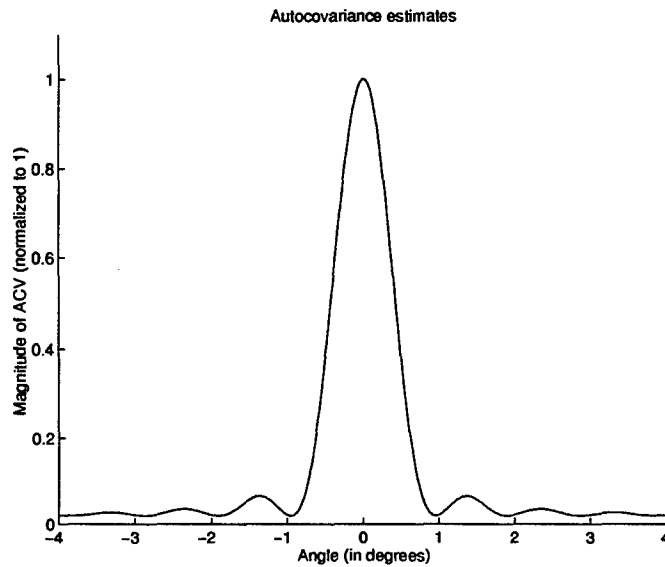


Figure 2.2 Theoretical Autocovariance (ACV) for 30λ square target, 50 scatterers.

This theoretical autocovariance estimate is plotted in Fig. 2.2. We can vary the number of scatterers or the target size, keeping a uniform distribution of scatterers. The number of scatterers only determines the depth of the first null, $\frac{1}{N}$. The width of the main lobe varies inversely with target size. A small target would tend to have the same RCS over a wider range of angles, and thus would produce a wider autocovariance main lobe. The RCS of a large target would vary more over a shorter range of angles so the RCS would decorrelate quicker. The theory also assumes independent scatterers. These are the three characteristics that we will vary in order to characterize the theory. The next chapter describes how we will generate our data based autocovariance results.

III. Measurement Procedure

3.1 Motivation for Static Measurements

We need to find the RCS autocovariance in order to determine P_D . From the previous chapter, we can generate a theoretical autocovariance sequence for a given distribution of scatterers. The next problem is to generate a data based autocovariance for a static measurement. The AFIT range was used to make all the RCS measurements, and its specifications are described in appendix A.

3.2 Generating Data Based Autocovariance

The procedure for generating a data based autocovariance is as follows:

1. Generate the locations for the point scatterers
2. Take azimuth sweep of static RCS data over 360°
3. Calculate autocovariance for this RCS data

In order to use a static measurement to validate the theory, we need to make a static RCS measurement that incorporates the same parameters as the ones input into the theory. Recall that to calculate the theoretical autocovariance the following are required:

1. equal amplitude scatterers
2. wavelength (λ)
3. number of scatterers
4. target distribution (size of target)
5. independent scatterers

Each of these parameters is explained below in order.

1. The scatterers are thin cylinders with height=10cm and radius=1.5mm. The cylinders appear to be isotropic scatterers when they are viewed from the side and rotated about the main axis. All the cylinders are the same size, so we have equal amplitude, isotropic scatterers.
2. Wavelength comes from the frequency of the incident wave. The wavelength is determined by the frequency which we choose based on the target size.
3. The number of scatterers is a characteristic we want to investigate. Holding the target distribution and wavelength constant, we will vary the number of scatterers.
4. Target size is another characteristic of interest. We will vary target size, holding the number of scatterers and distribution constant.
5. We also want to validate the assumption of independent scatterers. We will vary the spacing between scatterers, holding the number of scatterers and distribution constant.

3.3 Setting Up the Static Measurements

We want to place the scatterers, take an RCS azimuth sweep, calculate the autocovariance, and compare the resulting data based autocovariance estimate to a theory based estimate. We start with a 2.5' by 2.5' piece of styrofoam which will hold the cylinders upright and in place during the azimuth sweep. The styrofoam appears transparent at high frequencies and has an RCS of approximately -60dBsm. All of the measurements are at least 20dBsm above the styrofoam. On the styrofoam we drew a 60cm by 60cm grid with 21 lines on each side. The vertices represent locations where we can place the scatterers. This leads to 441 possible locations for the scatterers (see Fig. 3.1). For each measurement we need the number of scatterers, target size, and target distribution. The number of scatterers can range from 1 to 441. Target size must be between 1.5λ and 36λ . Any distribution that we can realize with the grid and point scatterers is possible. Once we have the number of scatterers, location, and distribution, we place the cylinders in the styrofoam and take a 360° azimuth sweep. An example of the RCS data is shown in Fig. 3.2. The data is

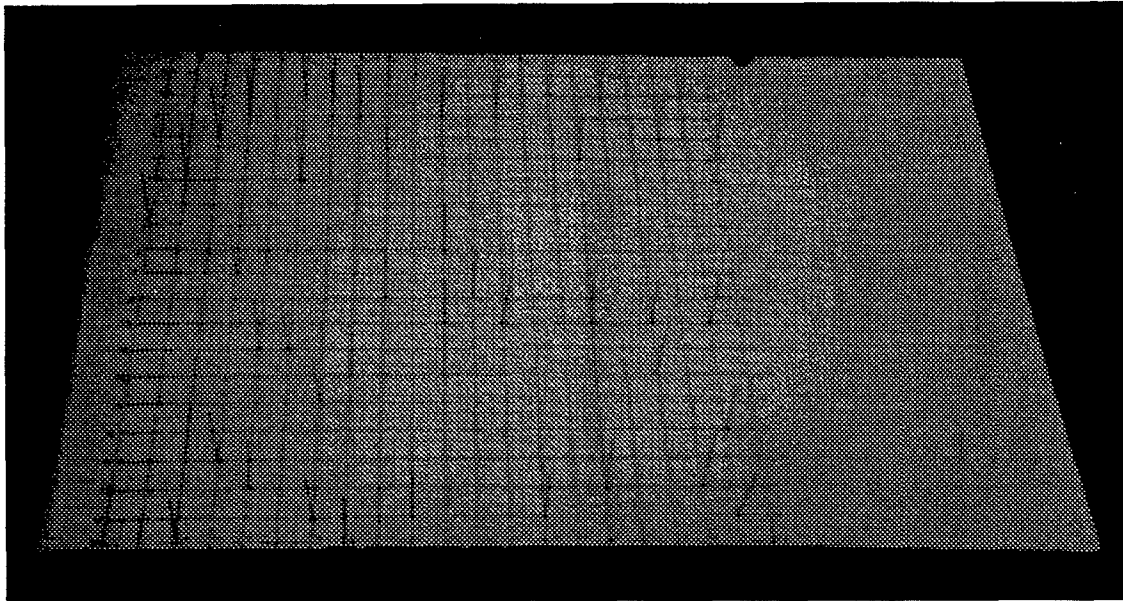


Figure 3.1 Static measurement setup - styrofoam with thin cylinders placed on grid.

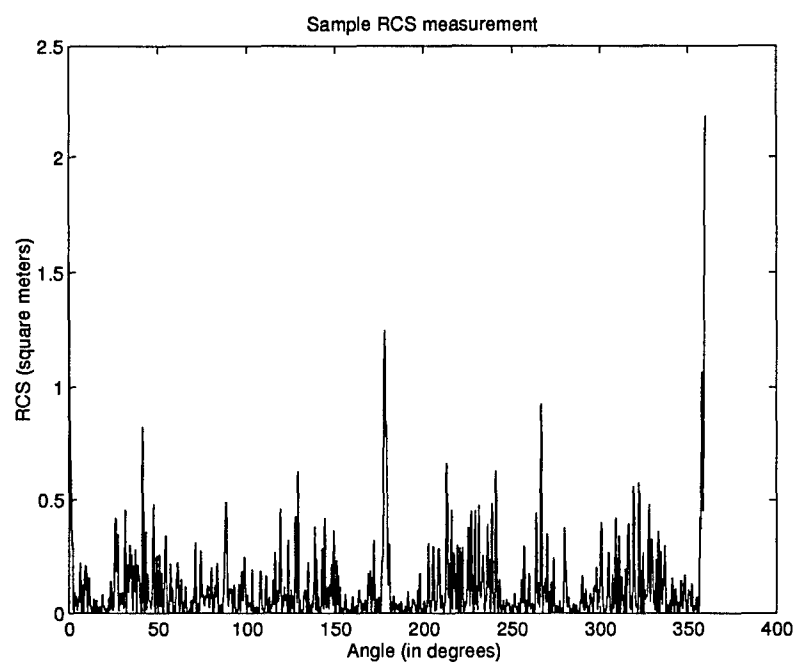


Figure 3.2 Sample RCS azimuth sweep - 100 scatterers, 30λ square

highly fluctuating. If this were the RCS data of an aircraft, a pulsed radar would not see 100% or 0% pulse to pulse correlation. Taking the autocovariance of this data and normalizing to one yields the following autocovariance sequence, shown in Fig. 3.3. We are only concerned with the

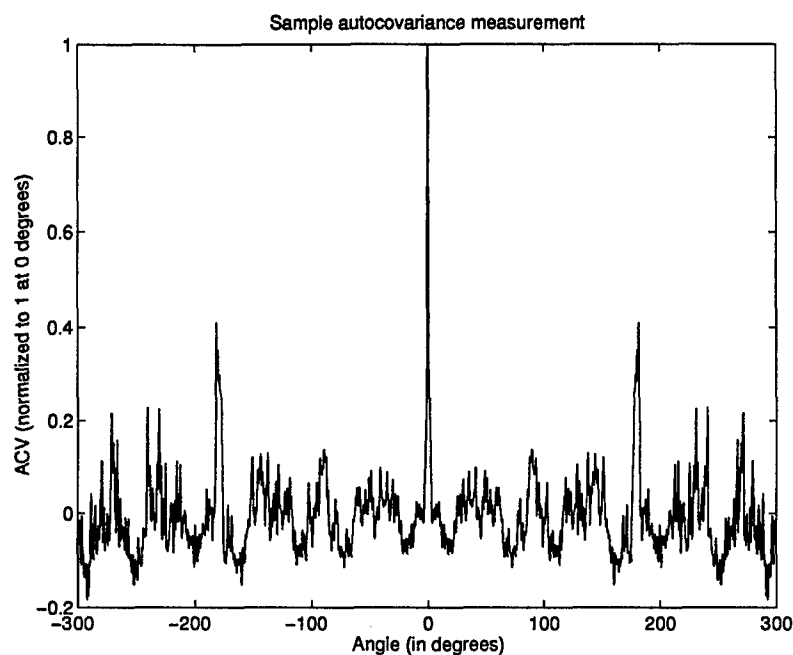


Figure 3.3 Sample data based autocovariance estimate

main lobe structure, so the rest of the data can be truncated. Figure 3.4 shows only the main lobe of the autocovariance. The resulting data based autocovariance curve can be compared to theory generated autocovariance curves for the same distribution, number of scatterers, and target size to validate the theory.

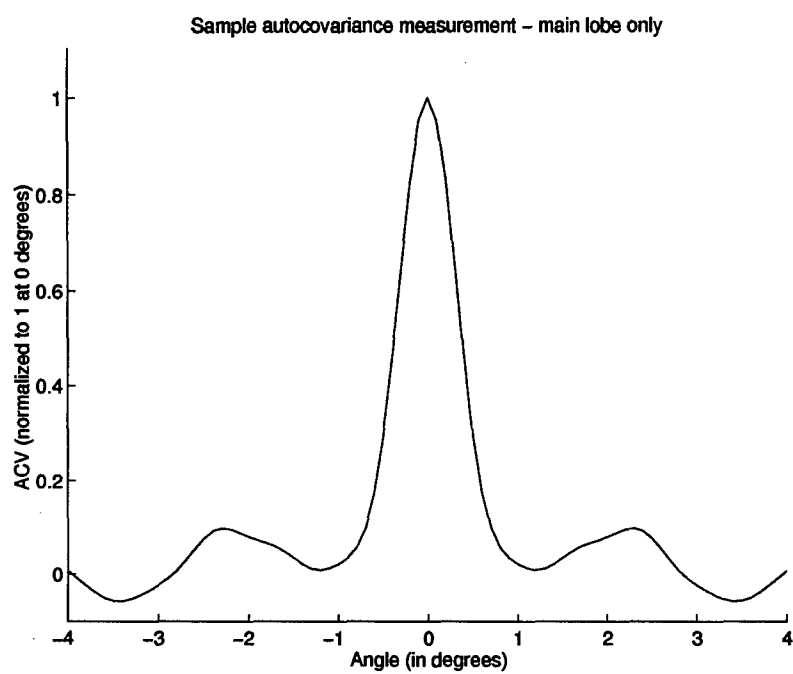


Figure 3.4 Main lobe of sample autocovariance

IV. Results

4.1 Data Matrix

Recall from Eqn. (2.9) that in order to calculate the autocovariance, we need the number of scatterers and the characteristic function of the target scatterer pdf. To calculate the latter, target size and wavelength are needed. Table 4.1 shows these input variables for each static measurement, along with which characteristic of the theory is being tested in the measurement. For each characteristic we will examine the following:

1. Why should we examine this characteristic?
2. How will we examine this characteristic?
3. What do we expect to find?
4. What do we find?

Table 4.1 Data matrix of static measurements used to characterize and validate theoretical autocovariance predictions

Variable	Target Size	Number of Scatterers	Distribution	Wavelength	Number of Realizations
Number of Scatterers	30λ	10	uniform	2cm	10
	30λ	50	uniform	2cm	9
	30λ	200	uniform	2cm	10
Target Size	14λ	50	uniform	4.3cm	10
	30λ	50	uniform	2cm	9
	36λ	50	uniform	1.7cm	10
Distance Between Scatterers	3λ	9	3 X 3	2cm	1
	12λ	9	3 X 3	2cm	1
	18λ	9	3 X 3	2cm	1
	30λ	9	3 X 3	2cm	1
	36λ	9	3 X 3	1.7cm	1

4.2 Varying Number of Scatterers

4.2.1 Motivation for Varying Number of Scatterers. Aircraft in flight may have different numbers of scattering centers when viewed from different angles. As the number of scattering

centers changes, the RCS return will also change. We do not need the exact number of scatterers to input into the theory, but we do need some number of scatterers for the theory. We want to know how the number of scatterers affects the autocovariance estimates.

4.2.2 How to Make the Measurements. The target size is fixed to 30λ by 30λ and the distribution is uniform. The number of scatterers is 10, 50, and 200. For the theory based autocovariance, we use exactly what is given above. The target pdf is a two dimensional rect function 30λ on a side, which means the characteristic function is a two dimensional sinc. The function $\text{rect}(x) = 1$ when $|x| < \frac{1}{2}$ and 0 elsewhere and $\text{sinc}(x) = \sin(\pi x)/(\pi x)$. The results are similar to those found in section 2.4. For the data based measurement, we randomly place with uniform probability the number of scatterers we want in the 21 by 21 grid. This measurement represents one realization. An azimuth sweep of RCS is taken, and the autocovariance can be calculated from this RCS data. In a uniform distribution, each scatterer is equally likely to be in any position within the distribution. When we average the results, we are letting the scatterers take on more positions within the target area. Now the scatterer locations appear more like a uniform distribution. For each data based autocovariance result, many measurements are averaged so that the deviation among all the autocovariance estimates is small.

4.2.3 Expected Results. According to the theory, the number of scatterers only affects the depth of the nulls, $\frac{1}{N}$. But the scatterers are not independent and a higher number of scatterers in a given target size should exhibit more interactions. Interactions occur when the incident wave bounces from one scatterer to at least one other before being captured by the receiving antenna. The theory assumes independent scatterers, or that the total RCS return is the sum of each individual return with no interactions. This will cause the autocovariance for a larger number of scatterers to agree less with the theory than for a smaller number of scatterers. The next subsection explains the reason why more interaction causes the main lobe of the autocovariance to broaden.

4.2.4 *Results.* As expected, the predicted results show approximately the same width of the main lobe with deeper nulls for larger number of scatterers. These results are shown in Figs. 4.1 to 4.3. For data based autocovariance, as the number of scatterers increases, the main lobe widens. Table 4.2 compares the main lobe widths using Full Width Half Max (FWHM). FWHM is the degree range spanned by an autocovariance greater than or equal to 0.5 where the autocovariance has been normalized to 1 at zero degrees. With more scatterers, interaction among scatterers causes the target to appear more like one large scatterer. The RCS is no longer a deterministic number that can be calculated from summing the individual returns at discrete locations. What we varied was the number of scatterers, but density can be expressed as number of scatterers per square wavelength, so we are also varying density. Note that it is not a large number of scattering centers that causes the main lobe to widen. A higher density of scatterers per square wavelength is the cause for the data based estimate to have a wider autocovariance main lobe than the predicted autocovariance.

Table 4.2 FWHM when varying the number of scatterers

Number of Scatterers	10	50	200
Predicted FWHM	0.91	0.86	0.85
Data Based FWHM	0.84	1.06	1.85
Difference	0.07	0.20	1.0
% Difference	8.6	19.3	54.1

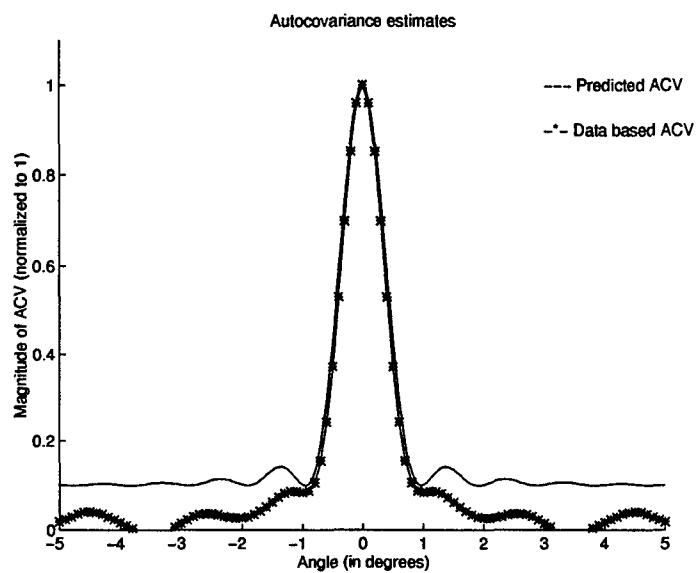


Figure 4.1 10 scatterers, 30λ square, average of 10 realizations

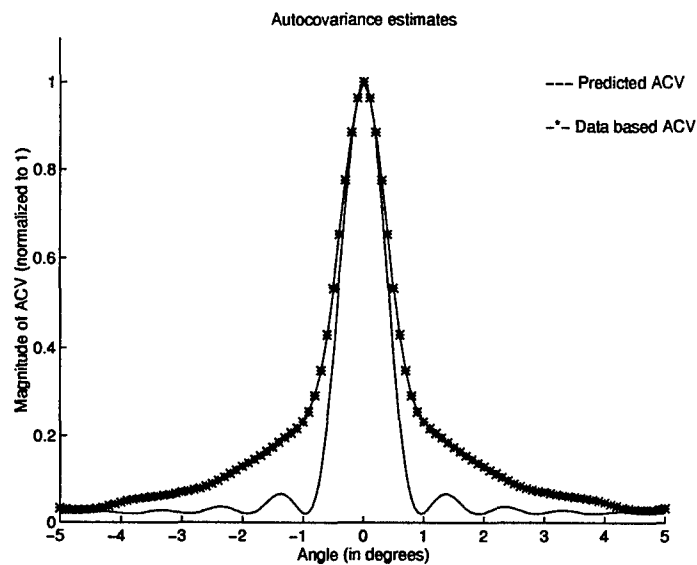


Figure 4.2 50 scatterers, 30λ square, average of 9 realizations

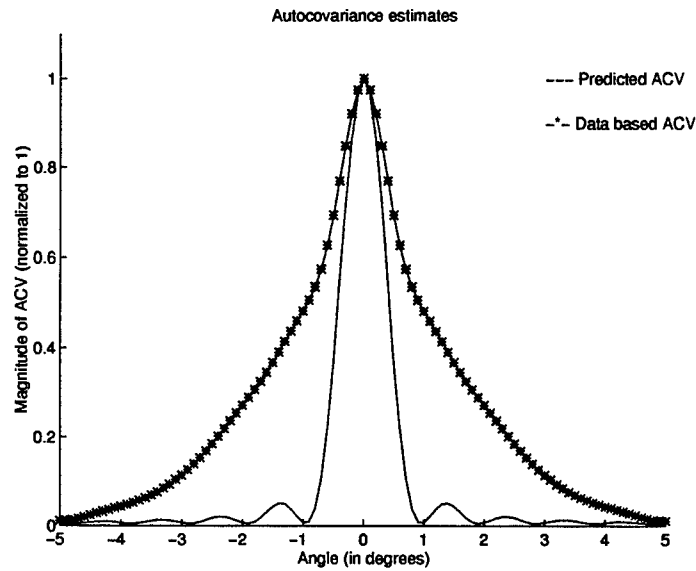


Figure 4.3 200 scatterers, 30λ square, average of 10 realizations

4.3 Varying Target Size

4.3.1 Motivation for Varying Target Size. Aircraft vary in size from a small aircraft like the C-29 (wingspan=15.66m) (6) to a large aircraft like the B-52 (wingspan=56.39m) (5). Also, a single aircraft may look very different in size from two different views. An example is the TU-160 Blackjack bomber. From a nose view, this aircraft has a width of 35.60m with wings swept, while from a side view the width is 54.10m (5). We want to know if the theory is valid for varying target sizes.

4.3.2 How to Make the Measurements. The number of scatterers is fixed at 50, and the distribution is still uniform. The target scatterer pdf is still a 2-D rect uniformly filled with scatterers, but of sizes 14λ , 30λ , and 36λ . A change in frequency is used to scale the electrical target size. To simulate a uniform distribution, 10 realizations are averaged together. The same scatterer distributions are used at each of the three target sizes.

4.3.3 *Expected Results.* With the number of scatterers constant, the main lobe null should be at the same depth for each measurement, $\frac{1}{50}$. From chapter II, a smaller target should have a wider autocovariance main lobe.

4.3.4 *Results.* The data and theory based autocovariances do exhibit a wider autocovariance main lobe for a smaller target size in Figs 4.4 to 4.6. The percent difference between theory and data based FWHM is not much different for this range of target sizes, varying from 9.3% to 19.3%, as shown in table 4.3.

Table 4.3 FWHM when varying target size

Target Size (λ)	14	30	36
Predicted FWHM	1.84	0.86	0.72
Data Based FWHM	2.16	1.06	0.79
Difference	0.32	0.21	0.07
% Difference	14.8	19.3	9.3

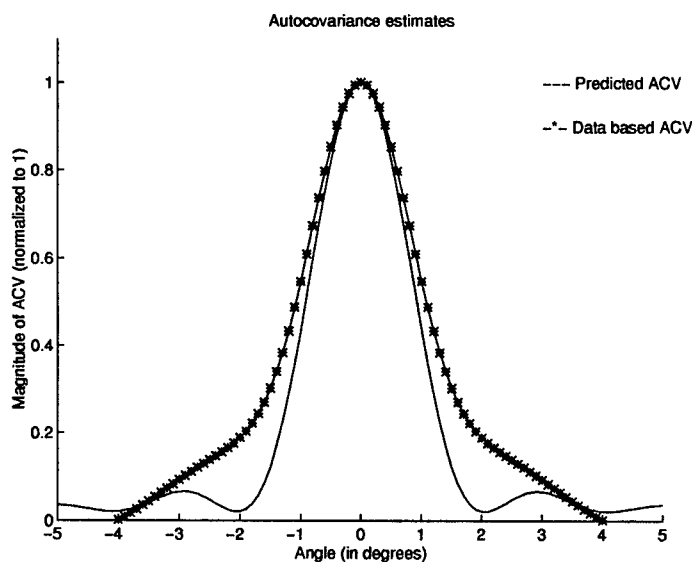


Figure 4.4 50 scatterers, 14λ square, average of 10 realizations

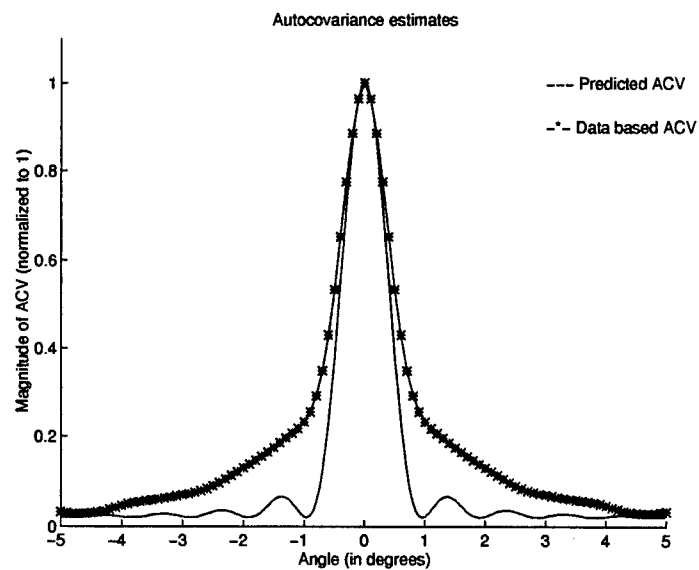


Figure 4.5 50 scatterers, 30λ square, average of 9 realizations

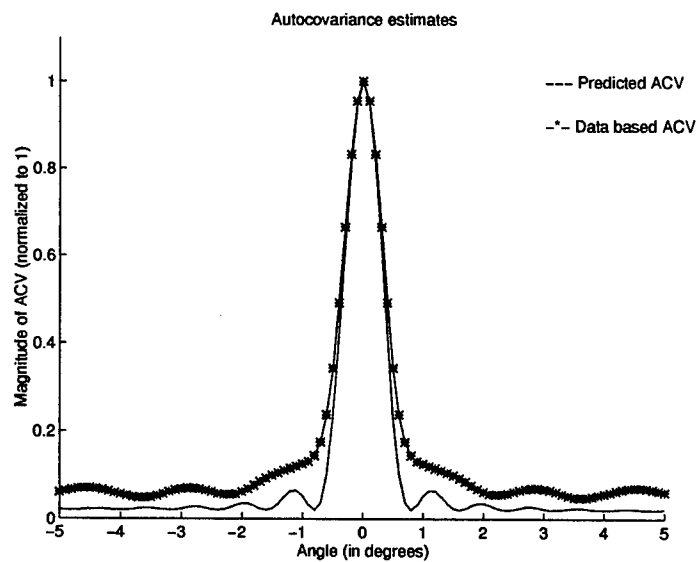


Figure 4.6 50 scatterers, 36λ square, average of 10 realizations

4.4 Varying Spacing Between Scatterers

4.4.1 Motivation for Varying Spacing Between Scatterers. Scatterer interaction is not accounted for in the theory. Instead, all scatterers are assumed to be independent. In section 4.2, the interaction of scatterers leads to errors in the theory based estimate. Now we want to characterize this error.

4.4.2 How to Make the Measurements. In this case, we keep the distribution and number of scatterers constant, varying the spacing between scatterers. Since we want the spacing between scatterers in one measurement to be the constant, we use the distribution of 9 discrete point scatterers shown in Fig. 4.7, which can easily be entered into the theory. D is the total target size in wavelengths and d is the distance between scatterers. Table 4.4 shows the frequency and spacing between scatterers for these measurements. Each single measurement based autocovariance

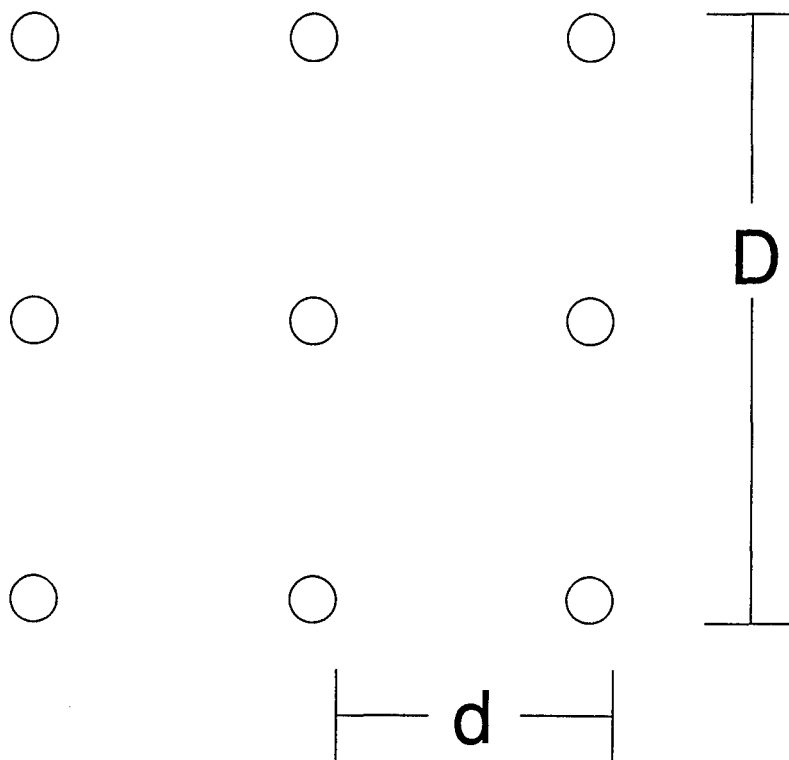


Figure 4.7 Target scatterer distribution for validating independence of scatterers.

estimate is compared to a theory based estimate.

Table 4.4 9 discrete point scatterer test frequencies and spacing

Frequency (GHz)	7	15	18
d (λ)	7	15	18
D (λ)	14	30	36

4.4.3 Expected Results. We expect the main lobe width to vary inversely with the total target size, D . If no interaction were present, we would find that the difference in data based and theory based results would be the same for each target size. For the predicted autocovariance, we expect the peaks that are not at 0 degrees to be almost as high as the main peak since the target scatterer pdf is very regular and deterministic.

4.4.4 Results. As expected, the smaller the target size D , the wider the main lobe on the autocovariance. Note that the range of angles on the X-axis is not the same on each plot in Figs. 4.8 to 4.12. We do not see any trend in the percent difference between data based and predicted FWHM when the spacing between scatterers is varied. This is probably due to the small number of scatterers. Even with a close spacing like 1.5λ , there is not enough interaction to make the data based results differ significantly from the predicted results. Due to the small number of scatterers, these results should be questioned. Independence of scatterers is better shown in section 4.2 where the density of scatterers per square wavelength was varied.

Table 4.5 FWHM when varying spacing between scatterers

Target Size (λ)	3	12	18	30	36
Predicted FWHM	9.18	2.29	1.53	0.92	0.76
Data Based FWHM	6.75	1.56	0.95	0.67	0.57
Difference	2.43	0.73	0.58	0.24	0.20
% Difference	36.0	46.5	60.2	36.0	34.6

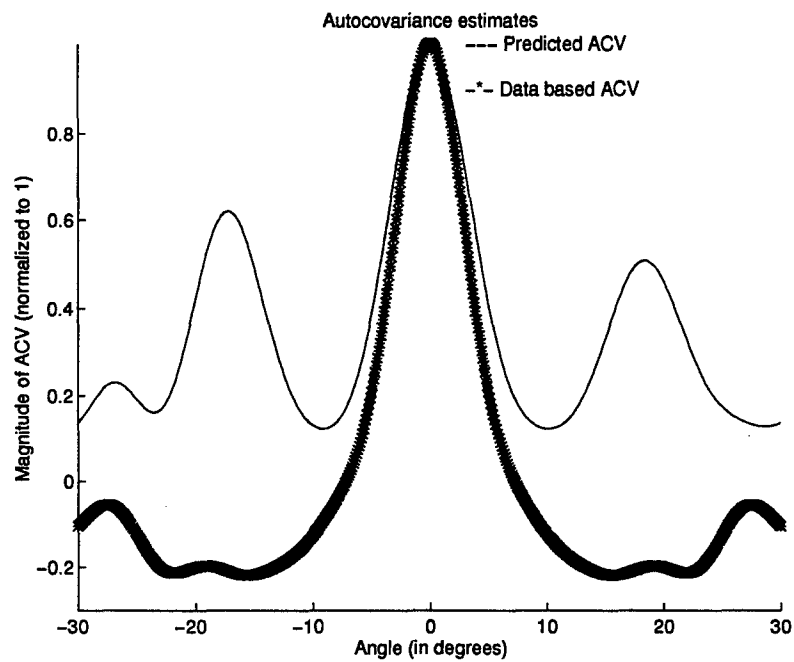


Figure 4.8 9 scatterers, 3λ square, 1 realization

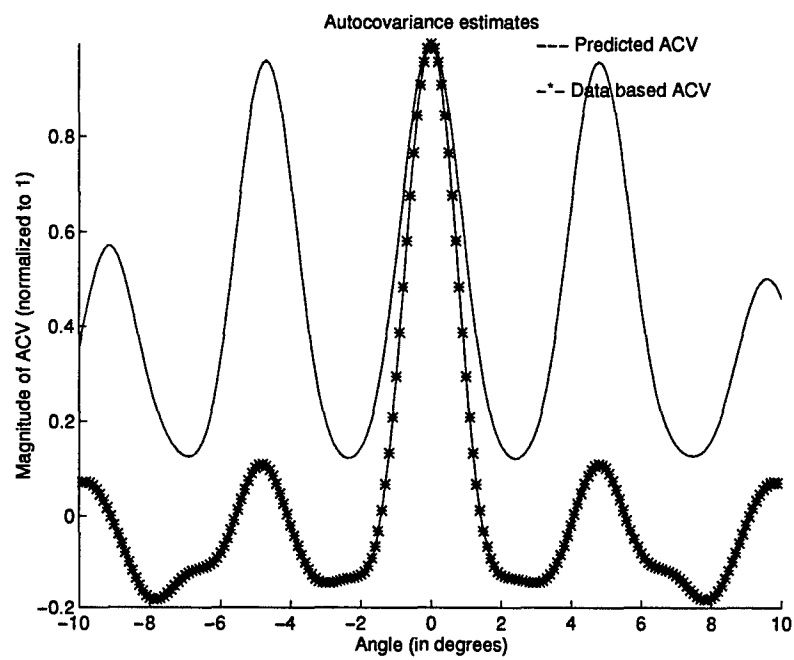


Figure 4.9 9 scatterers, 12λ square, 1 realization

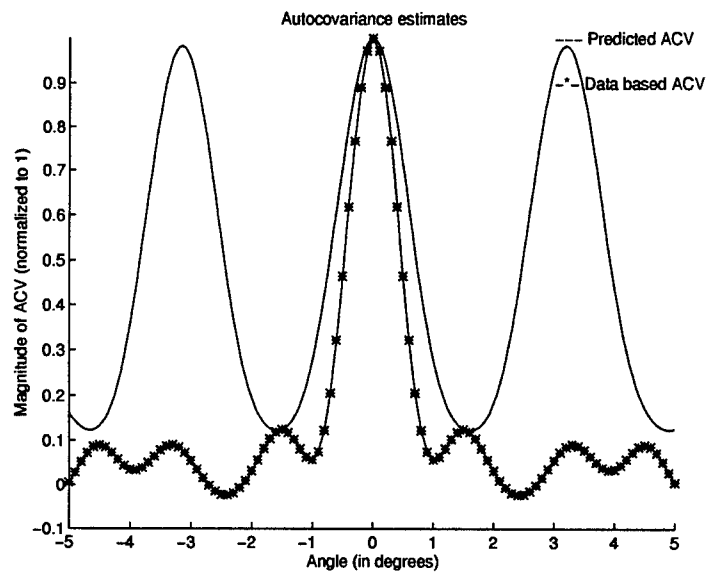


Figure 4.10 9 scatterers, 18λ square, 1 realization

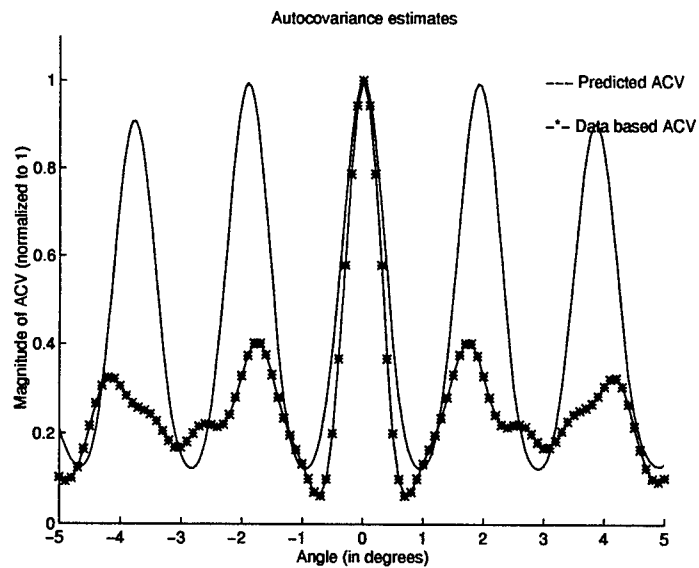


Figure 4.11 9 scatterers, 30λ square, 1 realization

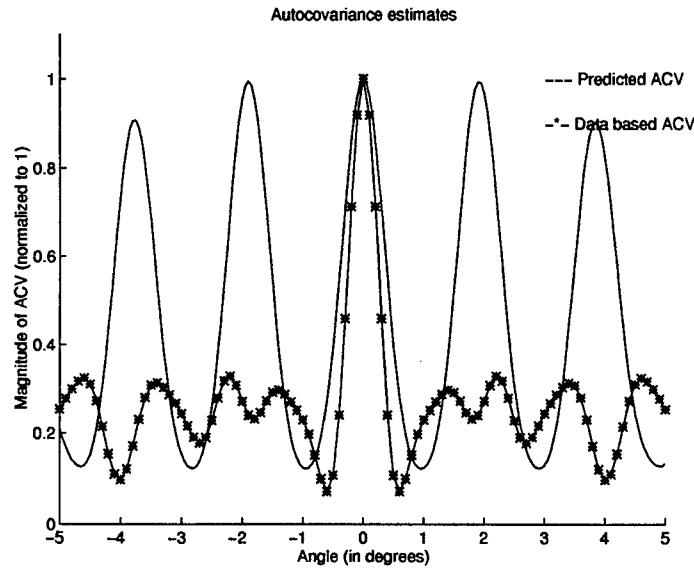


Figure 4.12 9 scatterers, 36λ square, 1 realization

4.5 Summary

In this chapter we looked at three variables of the autocovariance generating theory: number of scatterers, target size, and spacing between scatterers. In varying the number of scatterers, we were also varying the density. A higher density of scatterers per square wavelength leads to more interaction among scatterers which the theory does not account for. In the target size measurements, the results were as expected, that the RCS of a larger target will decorrelate faster in space than for a smaller target. Finally, the measurements for spacing did not contain enough scatterers to see the interactions we expected. These spacing measurements did confirm the same trends stated above about how target size relates to RCS decorrelation rate. The next chapter summarizes the conclusions of this research.

V. Conclusions and Recommendations

5.1 Conclusions

We can calculate the spatial autocovariance for a given target scatterer distribution and wavelength. When calculating the autocovariance, density of scatterers, wavelength, target size and target scatterer distribution are needed to determine the autocovariance main lobe width. The main lobe width, along with the rate at which the aircraft is changing aspect angle, leads to P_D for a pulsed radar. We need to consider the following in the calculation of the autocovariance:

1. The number of scatterers is not significant if we are only looking at the main lobe of the autocovariance. The number of scatterers determines the depth of the nulls in the autocovariance curves and if we are looking only at the main lobe, the null depth is not needed. The number of scatterers by itself did not affect the main lobe in Figs. 4.1 to 4.12.
2. The density, or number of scatterers per square wavelength, is very important. Since the theory does not account for interaction among scatterers, a high density of scatterers that are interacting will lead to autocovariance estimates that decorrelate much slower than the theoretical autocovariance predictions. Assuming independent scatterers causes problems in predicting the spatial autocovariance since the main lobe of the autocovariance widens with more interactions. Interactions among scatterers will lead to a wider autocovariance main lobe than what the theory predicts. Figures 4.1 to 4.3 and table 5.1 show this trend, that a higher density of scatterers leads to a wider autocovariance main lobe than predicted.

Table 5.1 Effects of varying density of scatterers on ACV main lobe

Density of Scatterers	0.011	0.056	0.222
Predicted FWHM	0.91	0.86	0.85
Data Based FWHM	0.84	1.06	1.85
% Difference	8.6	19.3	54.1

3. Spatial target size affects the width of the autocovariance main lobe. Large targets will have a narrower autocovariance main lobe and the RCS will decorrelate quicker than for a smaller target, as seen in Figs 4.4 to 4.6.

5.2 Recommendations

The theory in its most general form accounts for time effects as well as a bistatic radar situation. Testing and validation of the theory could be conducted with dynamic data to include time effects. In addition, a bistatic setup could be used to characterize the theory's bistatic results. We now know that for spatial correlations, interaction is the most significant source of error in the theory. Interaction could be incorporated into the theory to eliminate this error.

Appendix A. Specifications for the AFIT anechoic chamber

A.1 Specifications

Range Type: Non-compact

Frequency Range: 6.2GHz - 18.2GHz

Polarizations: V-Pol, H-Pol

Downrange Quiet Zone (amplitude, 1dB): 3.3'

Crossrange Quiet Zone (22.5° phase error): 1.5' @ 6.2GHz to 0.85' @ 18.2GHz

Noise Floor: -80 dBsm @ 6.2 GHz to -60dBsm @ 18.2GHz

Appendix B. Data Collection Procedure

For any given data set, the following is the procedure used to generate static RCS autocovariance measurements.

1. Generate scatterer locations
2. Take data
3. Convert raw data file to matlab matrix
4. Calculate autocovariance
5. Calculate average autocovariance (if needed)
6. Calculate predicted autocovariance
7. Plot predicted and data based results on one graph
8. Calculate figures of merit

I used matlab to generate all of my results. The data sets were treated as matrices at each step and saved in the matlab data files.

B.1 Generating scattering locations

First, I need to determine where to place the scatterers. For any measurement, I determine the number of scatterers (1-441). Matlab generates this many random numbers from 1-441, with uniform distribution. When the required number of scattering locations are selected, the result is converted from a 1 X 441 matrix to a 21 X 21 matrix, shown in Fig. B.1. Scatterers are placed in the styrofoam at these locations.

B.2 Taking data

With the scatterers in place in the styrofoam, I perform an azimuth sweep over 360° at $.1^\circ$ intervals. The data is saved as an ascii text file. The format is 79 header lines and then data.

```

1 1 1 0 0 0 0 1 0 1 1 1 0 0 1 1 0 1 1 0 0
1 0 0 0 0 1 0 0 1 1 0 0 0 0 1 0 1 1 0 0 0
0 1 0 1 1 1 1 1 0 1 1 1 0 1 0 0 0 0 1 0 0
1 0 1 0 0 1 1 0 0 0 0 1 0 0 1 1 0 1 0 0 1
1 0 0 0 1 1 0 1 0 0 0 0 0 1 1 0 0 0 0 0 1
1 1 0 1 0 0 0 1 0 0 1 1 1 0 1 0 0 0 1 1 0
0 1 0 0 0 0 1 1 1 1 0 0 0 0 1 0 1 1 1 1 1
1 0 0 1 1 0 1 0 0 0 1 0 1 1 0 0 1 0 0 0 1
1 1 1 1 1 0 1 0 1 1 1 1 0 0 1 0 1 0 0 0 1 1
0 0 1 0 1 0 0 0 0 0 0 0 0 1 0 0 1 1 0 0 0
0 0 1 0 1 0 1 1 0 1 1 1 1 0 1 0 0 1 0 0 0
1 0 1 0 1 1 1 0 1 0 0 0 0 1 1 1 1 0 1 0 0
0 1 1 0 0 1 0 0 0 0 0 1 0 0 1 0 0 1 1 0 1
0 0 0 1 1 0 1 1 1 1 0 0 0 0 1 0 0 1 0 1 0
0 0 0 0 0 0 0 1 0 1 1 0 1 0 1 1 1 1 0 0 1
1 0 1 0 0 1 1 1 1 1 0 1 0 1 0 1 0 0 1 1 0
0 1 1 0 1 1 0 0 0 0 1 0 1 0 1 0 1 0 0 1 1
0 1 0 1 0 0 0 1 1 1 0 0 0 0 1 1 1 0 1 1 0
1 0 1 0 0 0 1 0 0 1 1 1 0 0 1 0 1 0 0 0 1
1 1 0 0 0 0 0 1 1 1 1 0 1 0 0 1 0 1 0 0 0
1 0 0 1 0 1 0 1 0 0 1 0 0 0 1 1 1 1 0 1 0

```

Figure B.1 Example scattering locations generated from matlab for 200 scatterers

The header contains information such as frequency, data, polarization, etc. Each data point is in a three line format, as in the following:

DATA#0A

-8.561135, -47.3257

POS: 0.01 0.00 0.01 0.00 0.00 0.00

The second line is magnitude (dBsm) and phase of the RCS, while the first number after POS: is the angle.

B.3 Data preparation

Since I want to work with just the magnitude and angle, I use matlab to strip the header and extra text and write the magnitude (converted to m^2) and angle to a data file. I now have a 2 X 3600 data file which contains the magnitude in m^2 and angle for each RCS data point. An excerpt is shown below.

0.4082 0.4300

0.3113 0.5200

0.2247 0.6200

0.1840 0.7100

0.1657 0.8100

0.1669 0.9000

0.1825 1.0300

B.4 Finding autocovariance

I calculate the autocovariance of the RCS sequence. This generates a 2-3600-1 sequence of autocovariance and angle, part of which is shown below.

-0.9000 0.5597

-0.8000 0.5900

-0.7000 0.6283

-0.6000 0.6768

-0.5000 0.7355

-0.4000 0.8011

-0.3000 0.8681

-0.2000 0.9281

B.5 Taking average of autocovariances

Each measurement represents only one realization, which is given from a deterministic distribution of scatterers. In order to simulate a uniform distribution, I take many data sets and average the autocovariances. The deviations are small when we average all the autocovariances.

B.6 Predicting autocovariance

Next we need a theory based autocovariance. Theory was discussed in chapter II. Predicted autocovariance is generated by substituting the target pdf, number of scatterers, and wavelength into Eqn. (2.9).

B.7 Plotting comparisons

Now the predicted and data based autocovariances are plotted on one graph, adjusted to show only the main lobe structure.

B.8 Figures of merit

Finally, we need some way to quantify the differences in autocovariances for predicted and data based results. The width of the main lobe is the most important factor in finding the pulse to pulse correlation, so I calculate the Full Width Half Max (FWHM) of the main lobe. FWHM is the degree range spanned by an autocovariance of .5 or greater.

Bibliography

1. Balanis, Constantine A. *Advanced Engineering Electromagnetics*. Wiley, 1989.
2. Buterbaugh, Alan. *The Detection and Correlation Modeling of Rayleigh Distributed Radar Signals*. MS thesis, Air Force Institute of Technology, 1992.
3. Fischer, Brian. *Characterization of Dynamic Radar Cross Section Measurements using the Second Order Moment*. MS thesis, Air Force Institute of Technology, 1992.
4. Kehr, Robert. *Characterization of the Dynamic Radar Cross Section Properties of the C-29 Aircraft using First and Second Order Statistical Moments*. MS thesis, Air Force Institute of Technology, 1993.
5. Lambert, Michael. *Jane's All the World's Aircraft*. Sentinel House, 1992.
6. Lambert, Michael. *Jane's All the World's Aircraft*. Sentinel House, 1995.
7. Noble, Michael. *Second Order Statistical Characterization of Statically and Dynamically Measured Radar Cross-Section*. MS thesis, Air Force Institute of Technology, 1994.
8. Swerling, Peter. "Probability of Detection for Fluctuating Targets," *IRE Transactions, IT* (1960).
9. Welsh, Byron, et al. "Statistical Correlation Properties of Complex Scattering Targets." WPAFB, OH, May 1992.

Vita

Lieutenant Shannon was born on 08 April 1970 at [REDACTED] NC. He attended North Carolina State University where he graduated in 1995 with a Bachelor of Science Degree in Electrical Engineering. Upon graduation, he accepted a commission in the United States Air Force. In June 1995, Lieutenant Shannon was assigned to the Air Force Institute of Technology, where he has pursued a Masters of Science Degree in Electrical Engineering.

Permanent address: [REDACTED]
[REDACTED] 2474 [REDACTED] 2474

REPORT DOCUMENTATION PAGE			Form Approved OMB No. 0704-0188	
Public reporting burden for this collection of information is estimated to average 1 hour per response, including the time for reviewing instructions, searching existing data sources, gathering and maintaining the data needed, and completing and reviewing the collection of information. Send comments regarding this burden estimate or any other aspect of this collection of information, including suggestions for reducing this burden, to Washington Headquarters Services, Directorate for Information Operations and Reports, 1215 Jefferson Davis Highway, Suite 1204, Arlington, VA 22202-4302, and to the Office of Management and Budget, Paperwork Reduction Project (0704-0188), Washington, DC 20503.				
1. AGENCY USE ONLY (Leave blank)	2. REPORT DATE December 1996	3. REPORT TYPE AND DATES COVERED Master's Thesis		
4. TITLE AND SUBTITLE Experimental Investigation of Radar Cross Section Spatial Correlation Properties for a Point Scattering Target		5. FUNDING NUMBERS		
6. AUTHOR(S) John David Shannon				
7. PERFORMING ORGANIZATION NAME(S) AND ADDRESS(ES) Air Force Institute of Technology, WPAFB OH 45433-6477		8. PERFORMING ORGANIZATION REPORT NUMBER AFIT/GE/ENG/96D-19		
9. SPONSORING / MONITORING AGENCY NAME(S) AND ADDRESS(ES)		10. SPONSORING / MONITORING AGENCY REPORT NUMBER		
11. SUPPLEMENTARY NOTES				
12a. DISTRIBUTION / AVAILABILITY STATEMENT Distribution Unlimited		12b. DISTRIBUTION CODE		
13. ABSTRACT (Maximum 200 words)				
<p style="text-align: center;">Abstract</p> <p>This research investigates the spatial correlation of RCS. In pulsed radar systems, probability of detection for partially correlated signals depends on the autocovariance of the target's RCS. The RCS changes pulse to pulse due to spatial and time fluctuations. Spatial fluctuation are due to the motion of all scatterers relative to the radar (i.e. changing aspect angle). Time fluctuations are due to relative motion of scatterers to each other (i.e. wings flexing, engines spinning). Theory developed at AFIT [9] can generate autocovariance estimates from a distribution of scatterers. Theory based autocovariance estimates are compared to static measurement based autocovariance estimates in order to validate this theory. Interaction among scatterers is the most significant source of deviation between theory and measurement based autocovariance estimates.</p>				
14. SUBJECT TERMS Radar Cross Section, Correlation, Autocovariance		15. NUMBER OF PAGES 50		
		16. PRICE CODE		
17. SECURITY CLASSIFICATION OF REPORT UNCLASSIFIED	18. SECURITY CLASSIFICATION OF THIS PAGE UNCLASSIFIED	19. SECURITY CLASSIFICATION OF ABSTRACT UNCLASSIFIED	20. LIMITATION OF ABSTRACT UL	